Surface Impedance of Superconductors*

PIOTR B. MILLER
Department of Physics, University of Illinois, Urbana, Illinois
(Received December 21, 1959)

A detailed calculation of the surface impedance of superconductors is given based on the general theory of the anomalous skin effect in normal and superconducting metals given by Mattis and Bardeen. It is found that there are large corrections to the extreme anomalous limit value of the superconducting to normal surface resistance ratio; corrections to the surface reactance ratio are much smaller. The theory is compared with recent experiments on the surface impedance of aluminum and of tin. It is found that the theory gives satisfactory agreement with experimental data on the surface impedance, both in absolute value and in its temperature and frequency dependence over a wide range of temperatures and frequencies.

THERE has been a large amount of recent experimental work on the surface impedance of superconductors, with special emphasis on Al and Sn.[1–8] The Bardeen-Cooper-Schrieffer theory of superconductivity[9] has shown good quantitative agreement with many of the experimental properties of superconductors and it is of some interest to extend this quantitative agreement to the surface impedance. Mattis and Bardeen, and independently Abrikosov, Gorkov, and Khalatnikov have derived a general theory of the anomalous skin effect in normal and superconducting metals based on the BCS model of the superconductor.[10–12] In this paper we use the Mattis-Bardeen theory to compute the surface impedance of superconductors and compare the results with experiment.

The general result of Mattis and Bardeen[10] may be conveniently written in terms of the Fourier components of current $\mathbf{j}(\mathbf{q})$ and vector potential $\mathbf{A}(\mathbf{q})$ by defining $K(q)$ as,

$$\mathbf{j}(\mathbf{q})=-c(4\pi)^{-1}K(q)\mathbf{A}(\mathbf{q}), \tag{1}$$

where

$$K(q)=\frac{-3}{c^2\hbar v_0\Lambda(0)}\int_0^\infty\int_{-1}^1 e^{iqRu}e^{-R/l}(1-u^2)\times I(\omega,R,T)\,du\,dR, \tag{2}$$

and where the integration over u is the angular integration. Using the notation of reference 10, $I(\omega,R,T)$ may be written as:

$$\begin{aligned}I(\omega,R,T)=&-\pi i\int_{\epsilon_0-\hbar\omega}^{\epsilon_0}[1-2f(E+\hbar\omega)]\\&\times[g(E)\cos(\alpha\epsilon_2)-i\sin(\alpha\epsilon_2)]e^{i\alpha\epsilon_1}dE\\&-\pi i\int_{\epsilon_0}^{\infty}\{[1-2f(E+\hbar\omega)]\\&\times[g(E)\cos(\alpha\epsilon_2)-i\sin(\alpha\epsilon_2)]e^{i\alpha\epsilon_1}\\&-[1-2f(E)][g(E)\cos(\alpha\epsilon_1)\\&+i\sin(\alpha\epsilon_1)]e^{-i\alpha\epsilon_2}\}dE.\end{aligned} \tag{3}$$

The surface impedance is defined by

$$Z=R+iX=E(0)\left\{\int j(z)dz\right\}^{-1}. \tag{4}$$

For random scattering at the surface of the metal, the surface impedance is given by [9,13]

$$Z=-(4\pi^2i\omega/c^2)\left\{\int_0^\infty \ln[1+K(q)/q^2]dq\right\}^{-1}. \tag{5}$$

A simple approximation to the surface impedance given by (5) is the extreme anomalous limit approximation. Here one assumes that for all q of importance in the integral one has

$$q\pi\xi_0[\epsilon_0(0)/\epsilon_0]\gg1,\quad q\xi_0[\epsilon_0(0)/\hbar\omega]\gg1,\quad\text{and}\quad ql\gg1. \tag{6}$$

In this approximation,

$$K(q)\lambda_L^2(0)=\frac{3\pi\hbar\omega}{4\epsilon_0(0)q\pi\xi_0}\left(i\frac{\sigma_1}{\sigma_N}+\frac{\sigma_2}{\sigma_N}\right), \tag{7}$$

where σ_1/σ_N and σ_2/σ_N are the integrals given by

* This work was supported in part by the Office of Ordnance Research, U. S. Army.

[1] M. A. Biondi and M. P. Garfunkel, Phys. Rev. Letters **2**, 143 (1959); also Phys. Rev. **116**, 853 (1959); **116**, 862 (1959).
[2] R. Kaplan, A. H. Nethercot, Jr., and H. A. Boorse, Phys. Rev. **116**, 270 (1959).
[3] M. D. Sturge, Proc. Roy. Soc. (London) **A246**, 570 (1958).
[4] C. J. Grebenkemper, Phys. Rev. **96**, 1197 (1954).
[5] E. Fawcett, Proc. Roy. Soc. (London) **A232**, 519 (1955).
[6] A. B. Pippard, Proc. Roy. Soc. (London) **A203**, 98 (1950).
[7] A. B. Pippard, Proc. Roy. Soc. (London) **A203**, 195 (1950).
[8] D. M. Ginsberg, P. L. Richards, and M. Tinkham, Phys. Rev. Letters **3**, 337 (1959).
[9] J. Bardeen, L. N. Cooper, and J. R. Schrieffer, Phys. Rev. **108**, 1175 (1957); hereafter called BCS.
[10] D. C. Mattis and J. Bardeen, Phys. Rev. **111**, 412 (1958).
[11] A. A. Abrikosov, L. P. Gor'kov, and I. M. Khalatnikov, J. Exptl. Theoret. Phys. (U.S.S.R.) **35**, 265 (1958) [translation: Soviet Phys.-JETP **35(8)**, 182 (1959)].
[12] I. M. Khalatnikov and A. A. Abrikosov, *Advances in Physics*, edited by N. F. Mott (Taylor and Francis, Ltd., London, 1959), Vol. 8, p. 45.
[13] R. B. Dingle, Physica **19**, 311 (1953).

TABLE I. The complex conductivity as a function of frequency and temperature.

$\epsilon_0(T)/kT$	$\hbar\omega/kT$	σ_1/σ_N	σ_2/σ_N	$\epsilon_0(T)/kT$	$\hbar\omega/kT$	σ_1/σ_N	σ_2/σ_N
A	0.0567A	0.00	55.4	4.99	0.285	0.149	54.4
A	0.0850A	0.00	36.9	4.99	0.428	0.122	36.3
A	0.113A	0.00	27.6	4.99	0.570	0.104	27.2
A	0.199A	0.00	15.8	4.99	0.998	0.0714	15.5
A	0.283A	0.00	11.0	4.99	1.43	0.0530	10.9
A	0.425A	0.00	7.30	4.99	2.14	0.0359	7.20
A	0.567A	0.00	5.43	4.99	2.85	0.0260	5.36
A	0.850A	0.00	3.52	4.99	4.28	0.0160	3.48
A	1.13A	0.00	2.53	4.99	5.70	0.0112	2.50
A	1.99A	0.00	1.03	4.99	9.98	0.00604	0.999
A	2.83A	0.424	0.419	4.99	14.3	0.434	0.414
Limit as $A \to \infty$							
3.33	0.198	0.596	49.7	2.50	0.160	1.064	42.6
3.33	0.297	0.505	33.2	2.50	0.239	0.923	28.4
3.33	0.396	0.444	24.9	2.50	0.319	0.822	21.4
3.33	0.692	0.326	14.3	2.50	0.558	0.632	12.5
3.33	0.990	0.257	10.1	2.50	0.798	0.513	8.74
3.33	1.48	0.186	6.70	2.50	1.20	0.389	5.89
3.33	1.98	0.143	5.01	2.50	1.60	0.308	4.43
3.33	2.97	0.0936	3.27	2.50	2.39	0.211	2.91
3.33	3.96	0.0673	2.35	2.50	3.19	0.155	2.09
3.33	6.92	0.0887	0.883	2.50	5.58	0.222	0.733
3.33	9.90	0.478	0.384	2.50	7.98	0.550	0.326
1.74	0.130	1.54	29.7	1.13	0.113	1.73	17.6
1.74	0.196	1.38	20.3	1.13	0.170	1.56	11.4
1.14	0.261	1.24	15.4	1.13	0.227	1.44	8.69
1.74	0.457	0.992	9.00	1.13	0.397	1.24	5.21
1.74	0.652	0.835	6.44	1.13	0.567	1.04	3.78
1.74	0.978	0.665	4.40	1.13	0.850	0.866	2.73
1.14	1.30	0.548	3.35	1.13	1.13	0.737	2.05
1.74	1.96	0.396	2.22	1.13	1.70	0.565	1.36
1.74	2.61	0.304	1.59	1.13	2.27	0.449	0.884
1.74	4.57	0.449	0.499	1.13	3.97	0.697	0.273
1.74	6.52	0.673	0.237	1.13	5.67	0.819	0.125
0.700	0.105	1.60	7.38	0.400	0.102	1.35	2.74
0.700	0.158	1.47	5.11	0.400	0.153	1.27	1.96
0.700	0.210	1.38	3.97	0.400	0.203	1.21	1.58
0.700	0.368	1.20	2.46	0.400	0.356	1.09	0.970
0.700	0.526	1.06	1.83	0.400	0.509	1.00	0.734
0.700	0.788	0.924	1.31	0.400	0.764	0.893	0.504
0.700	1.05	0.812	1.01	0.400	1.02	0.886	0.331
0.700	1.58	0.715	0.568	0.400	1.53	0.910	0.190
0.700	2.10	0.762	0.352	0.400	2.03	0.917	0.119
0.700	3.68	0.868	0.117	0.400	3.56	0.954	0.0406
0.700	5.26	0.921	0.057	0.400	5.09	0.975	0.019
0.300	0.101	1.25					
0.300	0.151	1.19					
0.300	0.202	1.14					
0.300	0.353	1.04					
0.300	0.504	0.972					
0.300	0.756	0.940					
0.300	1.01	0.944					
0.300	1.51	0.950					
0.300	2.02	0.958					
0.300	3.53	0.979					
0.300	5.04	0.987					

Mattis and Bardeen[10]:

$$\frac{\sigma_1}{\sigma_N}=\frac{2}{\hbar\omega}\int_{\epsilon_0}^{\infty}[f(E)-f(E+\hbar\omega)]g(E)dE+\frac{1}{\hbar\omega}\int_{\epsilon_0-\hbar\omega}^{-\epsilon_0}[1-2f(E+\hbar\omega)]g(E)dE, \quad (8)$$

$$\frac{\sigma_2}{\sigma_N}=\frac{1}{\hbar\omega}\int_{\epsilon_0-\hbar\omega,\ -\epsilon_0}^{\epsilon_0}\times\frac{[1-2f(E+\hbar\omega)](E^2+\epsilon_0^2+\hbar\omega E)}{(\epsilon_0^2-E^2)^{\frac{1}{2}}[(E+\hbar\omega)^2-\epsilon_0^2]}dE. \quad (9)$$

The second term of (8) does not appear unless $\hbar\omega>2\epsilon_0$ in which case the lower limit of the integral in (9) is $-\epsilon_0$ instead of $\epsilon_0-\hbar\omega$. Numerical values of the complex conductivity integrals are given in Table I.

From (5) and (7) we get,

$$Z_{\infty,s}/Z_{\infty,n}=[(\sigma_1-i\sigma_2)/\sigma_N]^{-\frac{1}{3}}, \quad (10)$$

where the subscript ∞ henceforth denotes the extreme anomalous limit approximation and s and n denote superconducting and normal states, respectively.

We wish to make a better approximation than the extreme anomalous approximation, since in general the conditions of (6) are not satisfied for all the q values of importance in the superconductor. For this purpose we observe that in most experiments on pure metals the mean free path, l, is greater than 10^{-3} cm. Also the detailed theory of the surface impedance in the normal state, including relaxation effects, has been given by Dingle.[13] His numerical results show explicitly that for microwave frequencies the surface impedance for $l=10^{-3}$ cm differs from the impedance at $l=\infty$ by the order or 3%. We expect approximately the same difference in the superconductor since the same factor $e^{-R/l}$ enters into the current density. This has been verified experimentally by Sturge,[3] since he found very little change in surface resistance between two different superconducting Sn specimens with $l=10^{-3}$ cm and $l=5\times10^{-3}$ cm. Also the effect on the static penetration depth of the $e^{-R/l}$ factor in the current density shows approximate agreement with experiment.[14] Thus we are justified in taking $l=\infty$ in the theory. Then we may carry out the angular integration in (2) to get

$$K(q)=\frac{12\pi i}{c^2\hbar v_0 q\Lambda(0)}\Big(\int_0^{\infty}\int_{\epsilon_0-\hbar\omega}^{\epsilon_0}[1-2f(E+\hbar\omega)]\times[g(E)\cos(\alpha\epsilon_2)-i\sin(\alpha\epsilon_2)]e^{i\alpha\epsilon_1}\times R(x)dxdE+\int_0^{\infty}\int_{\epsilon_0}^{\infty}\{[1-2f(E+\hbar\omega)]\times[g(E)\cos(\alpha\epsilon_2)-i\sin(\alpha\epsilon_2)]e^{i\alpha\epsilon_1}-[1-2f(E)][g(E)\cos(\alpha\epsilon_1)+i\sin(\alpha\epsilon_1)]\times e^{-i\alpha\epsilon_2}\}R(x)dxdE\Big), \quad (11)$$

where $x=qR$ and

$$R(x)=(1/x^2)[(\sin x/x)-\cos x]. \quad (12)$$

In doing the integrations of (11) we use the following definitions and lemmas:

$$F(a)\equiv\int_0^{\infty}\sin(ax)R(x)dx=\tfrac{1}{4}[2a+(1-a^2)\ln|(1+a)/(1-a)|], \quad (13)$$

$$G(a)\equiv\int_0^{\infty}\cos(ax)R(x)dx=0 \text{ for } a>1,\quad =(\pi/4)(1-a^2) \text{ for } a<1.$$

[14] P. B. Miller, Phys. Rev. 113, 1209 (1959).

A large part of the integration over x in (11) may be done exactly by using (13) and (14) but the subsequent integration over E cannot be performed exactly. However we may get approximate formulas for $K(q)$ by expanding in a power series in q. The integrations are lengthy so that only the final results are given. For large q we get

$$K(q)\lambda_L^2(0)=\frac{3\pi}{4q\pi\xi_0}\left\{\frac{\hbar\omega}{\epsilon_0(0)}\left[i\frac{\sigma_1}{\sigma_N}+\frac{\sigma_2}{\sigma_N}\right]-\frac{16}{\pi(q\pi\xi_0)}\frac{\epsilon_0^2}{\xi_0^2(0)}\left[\ln(q\pi\xi_0)-\left(\frac{\hbar\omega}{2\epsilon_0}\right)^2\right]\right\}$$

$$\text{for } (q\pi\xi_0)\epsilon_0(0)/\epsilon_0\gg 1 \text{ and } q\xi_0\epsilon_0(0)/\hbar\omega\gg 1. \quad (15)$$

Note that in the limit $\omega\to 0$, this reduces to the appropriate formula given by BCS. Also in the limit $\epsilon_0\to 0$, this reduces to the correct formula for the normal metal.

In the opposite limit of small q we find for the real part of $K(q)$:

$$K(q)_R\lambda_L^2(0)=1+\tfrac{1}{5}(q\pi\xi_0)^2\left(\frac{\epsilon_0(0)}{\hbar\omega}\right)^2\times\left(1+8\epsilon_0^2\int_{\epsilon_0}^{\infty}\frac{[f(E)-\frac{1}{2}]dE}{(E^2-\epsilon_0^2)^{\frac{1}{2}}(4E^2-\omega^2)}\right). \quad (16)$$

In the limit $\epsilon_0\to 0$ we get the correct equation for the normal state. Also for $T=0$ we get a result identical to that of Khalatnikov and Abrikosov.[12] Note that the leading term in (16) for small q gives the full London value for $K(q)$ with all the electrons being accelerated by the electric field. Equation (16) is clearly not valid for $\omega=0$. For the imaginary part we get

$$K(q)_I\lambda_L^2(0)=0 \quad \text{for } q<\omega/v_0 \text{ and } \hbar\omega<2\epsilon_0, \quad (17)$$

$$K(q)_I\lambda_L^2(0)=\frac{\epsilon_0^2(q\pi\xi_0)^2}{10\epsilon_0(0)[(\hbar^2\omega^2/4)-\epsilon_0^2]^{\frac{1}{2}}}\left(\frac{\epsilon_0(0)}{\hbar\omega}\right)^3\times[1-2f(\hbar\omega/2)]$$

$$\text{for } (q\pi\xi_0)\frac{\epsilon_0(0)}{(\hbar^2\omega^2-4\epsilon_0^2)^{\frac{1}{2}}}\ll 1 \text{ and } \hbar\omega>2\epsilon_0. \quad (18)$$

Note that for $q<\omega/v_0$ and $\hbar\omega<2\epsilon_0$ there is no absorption of energy by the electrons. This corresponds to the fact that a free electron cannot absorb a quantum unless the velocity of the electron is greater than the phase velocity of the wave. This follows directly from conservation of energy and momentum. For $\hbar\omega>2\epsilon_0$ there is an added absorption in the superconductor given by (18), this added absorption clearly being zero in the normal state. Equation (18) is derived from the following integral formula, valid for $q<\omega/v_0$:

$$K(q)_I\lambda_L^2(0)=\frac{3}{2(q\pi\xi_0)\epsilon_0(0)}\left\{\int_0^{\infty}\int_{\epsilon_0-\hbar\omega}^{\epsilon_0}[1-2f(E+\hbar\omega)]\left[[g(E)-1]\cos\left(\frac{x}{q\pi\xi_0}\frac{[(E+\hbar\omega)^2-\epsilon_0^2]^{\frac{1}{2}}-[E^2-\epsilon_0^2]^{\frac{1}{2}}}{\epsilon_0(0)}\right)\right.\right.$$
$$\left.\left.+[g(E)+1]\cos\left(\frac{x}{q\pi\xi_0}\frac{[(E+\hbar\omega)^2-\epsilon_0^2]^{\frac{1}{2}}+[E^2-\epsilon_0^2]^{\frac{1}{2}}}{\epsilon_0(0)}\right)\right]R(x)dxdE\right\}. \quad (19)$$

Term (19) only appears for $\hbar\omega>2\epsilon_0$. The physical interpretation of (19) is that a ground pair of the superconductor is broken up by the incoming photon of momentum $\hbar\mathbf{q}$ and the final state is that of two single particles. This interpretation may be justified in detail by writing (19) in the limit of small q:

$$K(q)_I\lambda_L^2(0)=\frac{3}{2}\frac{[1-2f(\hbar\omega/2)]}{(q\pi\xi_0)\epsilon_0(0)}\int_0^{\infty}\int_{-\gamma-(\hbar\omega/2)}^{\gamma-(\hbar\omega/2)}[g(E)-1]\cos\left(\frac{x}{q\pi\xi_0}\frac{[(E+\hbar\omega)^2-\epsilon_0^2]^{\frac{1}{2}}-[E^2-\epsilon_0^2]^{\frac{1}{2}}}{\epsilon_0(0)}\right)R(x)dxdE, \quad (20)$$

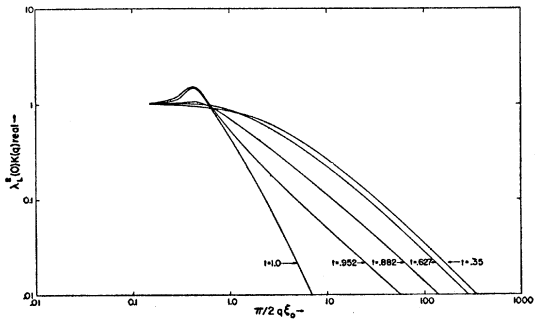

FIG. 1. The real part of $K(q)\lambda_L^2(0)$ is plotted versus $(\pi/2)q\xi_0$ for a frequency $\hbar\omega=1.5kT_c$, and for various reduced temperatures.

where

$$\gamma=[\epsilon_0(0)/\hbar\omega][(\hbar^2\omega^2/4)-\epsilon_0^2]^{\frac{1}{2}}(q\pi\xi_0). \quad (21)$$

We identify the dummy variable of integration E with one half of the negative of the energy needed to break up one ground pair

$$E=-(\epsilon_k^2+\epsilon_0^2)^{\frac{1}{2}}. \quad (22)$$

Then applying conservation of energy and momentum to the process we find that for a given q the maximum allowed range of E is

$$E=(-\hbar\omega/2)\pm\gamma \quad (23)$$

which agrees with the limits of integration in (20).

Furthermore we identify the factor $[1-2f(\hbar\omega/2)]$ of (20) as giving the probability of the initial state in the direct process and then subtracting the probability of the initial state in the inverse process. This extra absorption in the superconductor might give rise to a ratio R_s/R_n which is slightly greater than unity if appropriate conditions on frequency, temperature, and coherence distance were available.

All these results are summarized by plotting graphs of both the real and imaginary parts of $K(q)\lambda_L^2(0)$ versus $(q\pi\xi_0/2)$ (Figs. 1 and 2). The intermediate regions of q have been gotten by interpolation. We shall show that the surface resistance is sensitive to the exact shape of the $K(q)$ curves so that the interpolation method will introduce some lack of precision in the final numerical results for the surface resistance.

We have used graphs similar to those given in Figs. 1 and 2 to compute the surface impedance by numerical integration of (5). It is convenient to plot the results by giving the ratio r/r_∞, where r itself is the ratio of superconducting to normal surface resistance and where r_∞ is the ratio of superconducting to normal surface resistance computed in the extreme anomalous limit approximation. A similar plot is given for the surface

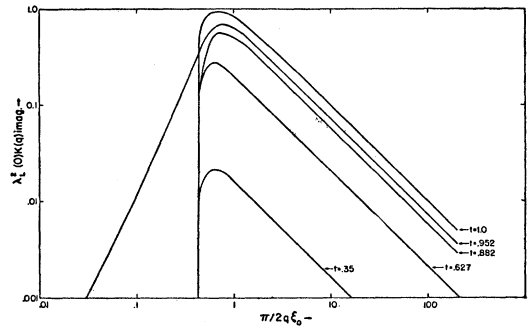

FIG. 2. The imaginary part of $K(q)\lambda_L^2(0)$ is plotted versus $(\pi/2)q\xi_0$ for a frequency $\hbar\omega=1.5kT_c$, and for various reduced temperatures.

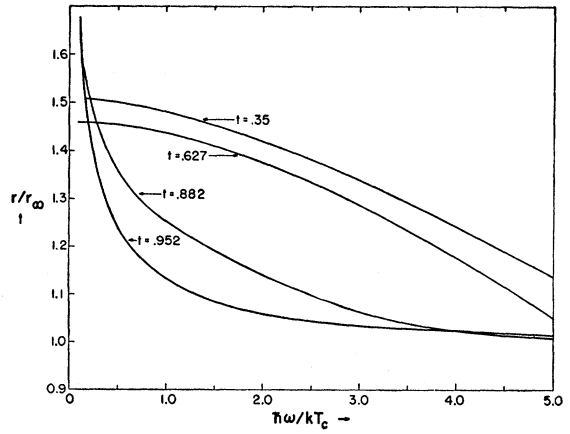

FIG. 3. The ratio r/r_∞ for Al is plotted versus reduced frequency $\hbar\omega/kT_c$ for various reduced temperatures.

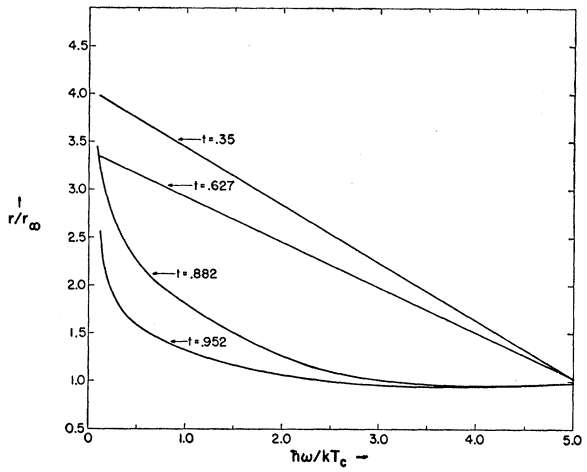

FIG. 4. The ratio r/r_∞ for Sn is plotted versus reduced frequency $\hbar\omega/kT_c$ for various reduced temperatures.

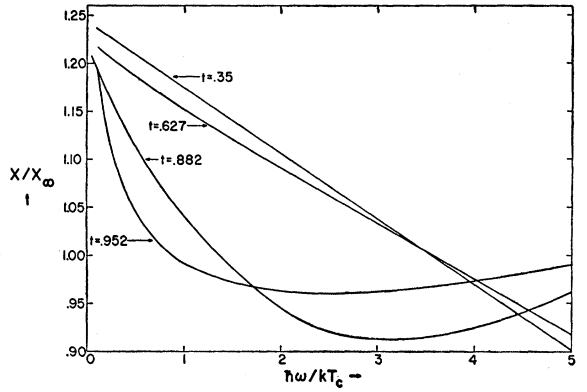

FIG. 5. The surface reactance ratio x/x_∞ for Sn is plotted versus reduced frequency $\hbar\omega/kT_c$ for various reduced temperatures.

reactance. Our numerical results for the normal state agree with the results of Dingle, which is to be expected since the two theories for the normal state are identical.[13] The results for Al and for Sn are shown in Figs. 3, 4, and 5. (The surface reactance ratio plot fo Al is not given here.)

We may understand the qualitative features of these results as follows. First we note that the corrections to the extreme anomalous limit are much larger for Sn than for Al due to the fact that the ratio $\xi_0/\lambda_L(0)$ is much larger for Al than for Sn.[9] Also for very high frequencies the ratios r/r_∞ and x/x_∞ approach unity in agreement with the similar behavior of the normal and superconducting states at very high frequencies. The large values of r/r_∞ and x/x_∞ at low frequencies near T_c arise from the large penetration depth which enhances the importance of small q values. The curves of Figs. 3, 4, and 5 are not very precise due to the interpolation procedure used in Figs. 1 and 2.

Biondi and Garfunkel have recently obtained accurate experimental data on the surface resistance ratio,

r, for Al over a wide range of frequencies and temperatures.[1] They have also calculated the skin depth in superconducting Al from the measured frequency dependence of the surface resistance ratio and the use of the Kronig-Kramers integral transforms.[1] By an approximate analysis of their data they find an energy gap at absolute zero of

$$E_g(0)=(3.25\pm0.1)kT_c. \tag{24}$$

Using the detailed theoretical results given by Fig. 3, we find best agreement with experiment for an average energy gap given by

$$E_g(0)=3.37kT_c, \tag{25}$$

and by assuming the same temperature dependence of the gap as the BCS theory. It has been shown that one may introduce an anisotropic energy gap into the BCS theory and that the only resulting change in the BCS theory is that the square of the energy gap $\epsilon_0^2(T)$ is everywhere replaced by $FF^*(\mathbf{k},T)$ where $\mathbf{k}$ is the momentum of the excitation.[15,16] This gives a natural justification for treating the energy gap as a parameter in the BCS theory.

The experimental curves given by Biondi and Garfunkel[1] together with the theoretical points computed assuming (25) are shown in Fig. 6. The agreement with experiment is quite good. The small deviations at low temperatures might possibly be due to anisotropy of the energy gap. The skin depth, δ_r, determined by Biondi and Garfunkel is also compared with the theoretical skin depth in Fig. 7. The energy gap of (25) has again been assumed in computing the theoretical skin depth. The theoretical curve was determined by use of curves for Al which are not shown here because the correction to x_∞ was only of the order of 5 %. Both energy-gap values (24) and (25) are in approximate agreement with other experiments on thermal conductivity[17] and on nuclear spin relaxation.[18]

The comparison of theory and experiment for Sn is carried out in a different way, mainly because most of the reliable experimental data lies well below the energy gap. The surface resistance of the normal state in Sn is highly anisotropic so that we compare the theory with results on polycrystalline specimens, or averaged single crystals. Many recent experiments have shown that at intermediate temperatures and in a large frequency range

$$(\hbar\omega\sim0.01kT_c \quad \text{to} \quad \hbar\omega\sim1.0kT_c)$$

the surface resistance ratio, r, may be written as[2-7]

$$r=\phi(t)A(\nu), \tag{26}$$

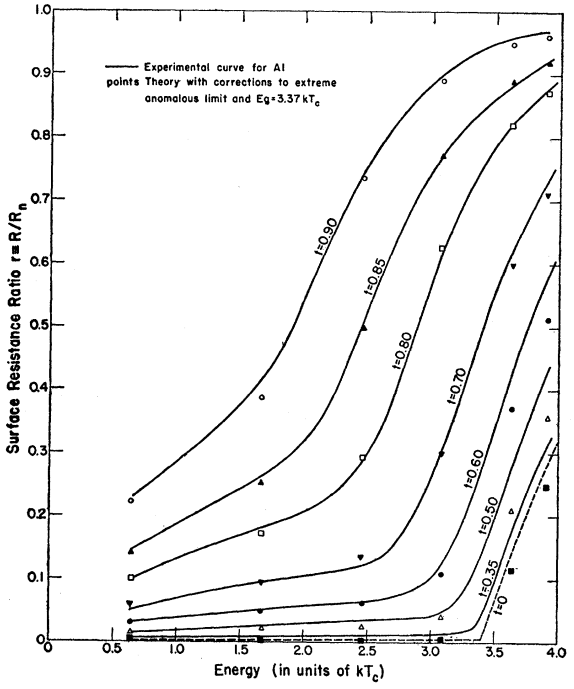

FIG. 6. The experimental curve of resistance ratio, r, for Al plotted versus reduced frequency for various values of reduced temperature (Biondi and Garfunkel). The dashed curve is the experimental data extrapolated to $T=0$. The theoretical points shown have been computed assuming an energy gap at $T=0$ of $3.37kT_c$. There are no theoretical points shown to correspond to the dashed curve at $T=0$.

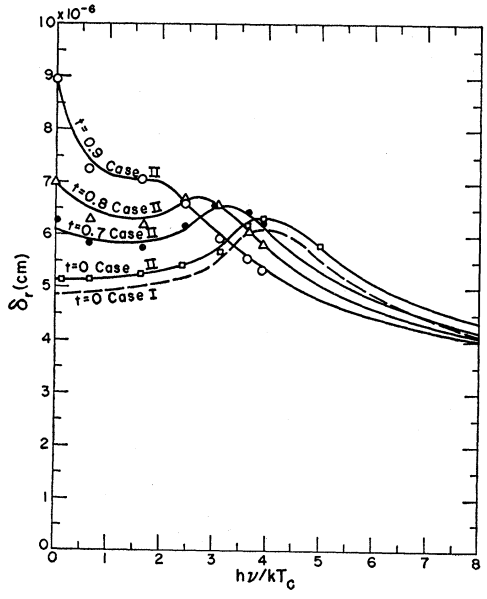

FIG. 7. The skin depth for Al, δ_r, is plotted versus the reduced frequency, $h\nu/kT_c$. The solid curves were gotten by Biondi and Garfunkel from their experimental data and use of the Kronig-Kramers integral transform. Case II refers to use of the detailed theory of Dingle for the normal state, Case I to the use of the extreme anomalous limit for the normal state. The points shown are the detailed theory of this paper with $E_g(0)=3.37kT_c$.

[15] L. N. Cooper, Phys. Rev. Letters **3**, 17 (1959).
[16] N. N. Bogoliubov, J. Exptl. Theoret. Phys. (U.S.S.R.) **34**, 58 (1958) [translation: Soviet Physics-JETP **34**, 41 (1958)].
[17] C. B. Satterthwaite, Cambridge Superconductivity Conference, 1959 (unpublished).
[18] A. G. Redfield, Phys. Rev. Letters **3**, 85 (1959).

where t is the reduced temperature. The experiments show that at intermediate temperatures the function $\phi(t)$ is

$$\phi(t)=t^4(1-t^2)/(1-t^4)^2. \quad (27)$$

The range of validity of the $\phi(t)$ law differs somewhat in different experiments but most of the data show that the $\phi(t)$ law is valid from approximately $t\sim0.4$ to approximately $t\sim0.8$.

We have compared the theoretical results with the temperature law of (27). We find that the $\phi(t)$ law is approximately valid to within about 10% in the following temperature and frequency range. It is valid from $\hbar\omega=0.01kT_c$ to $\hbar\omega=2kT_c$ and from $t\sim0.4$ to $t\sim0.7$. (The values for $\hbar\omega<0.12kT_c$ were obtained by an approximate extrapolation of the low-temperature curves of Fig. 2.) For low frequencies ($\hbar\omega\sim0.1kT_c$) the $\phi(t)$ law remains valid up to about $t\sim0.8$ as the uppper bound and the lower bound goes somewhat below $t\sim0.4$.

A large amount of data by different experimenters for $A(\nu)$ has been summarized in Fig. 8.[19] The data is for polycrystalline specimens or the appropriate average of single crystals. The figure also shows the results of the detailed theory and of the extreme anomalous limit theory. The detailed theory gives a curve which has a very similar shape to the experimental data but is roughly 25% greater in absolute value. The extreme anomalous theory differs in absolute value by a factor of about 2.5 from the experimental points. In view of the large anisotropy in the absolute value of $A(\nu)$ in Sn single crystals and several other complicating features of Sn such as an anisotropic energy gap,[20] the agreement

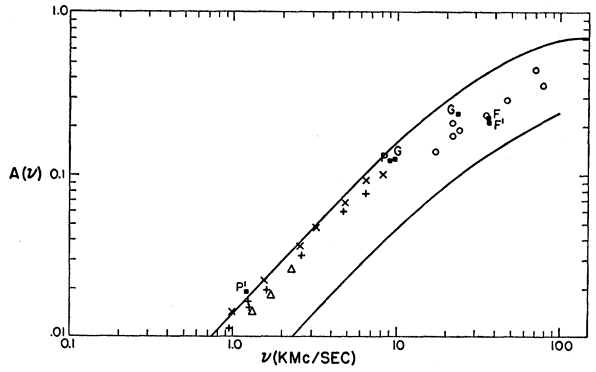

FIG. 8. $A(\nu)$, the frequency dependent part of r, as a function of frequency. ○—Kaplan et al (reference 2); ×, +, △—Sturge (reference 3) (three different averaged single crystals); P—Pippard (reference 6) (averaged single crystal); P'—Pippard (reference 7) (polycrystal); G—Grebenkemper (reference 4) (polycrystal); F—Fawcett (reference 5) (averaged single crystal); F'—Fawcett (polycrystal). The upper curve is the detailed theory of this paper. The lower curve is the extreme anomalous limit theory.

[19] The experimental points of this plot are reproduced from reference 2.

[20] R. W. Morse, T. Olsen, and J. D. Gavenda, Phys. Rev. Letters 3, 15 (1959).

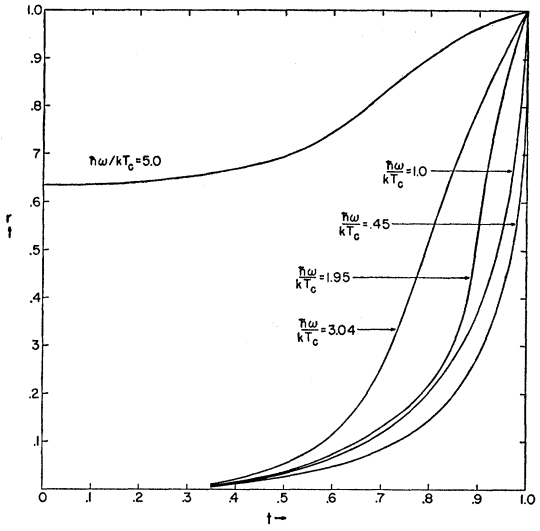

FIG. 9. The theoretical surface resistance of Sn is plotted versus reduced temperature in the high-frequency region.

with the detailed theory is satisfactory. Also the absolute value of $A(\nu)$ depends sensitively on the value of the parameter $\xi_0/\lambda_L(0)$ whereas the shape of the curve is approximately independent of this parameter.

We have plotted theoretical curves for the surface resistance ratio, r, for Sn at frequencies near the energy gap in Fig. 9. There does not seem to be any reliable experimental data in this frequency range. We have also plotted theoretical curves of the skin depth of Sn in Fig. 10. This curve was computed using the graphs of x/x_∞ given in Fig. 5. Qualitatively the skin depth of Sn behaves similarly to the curves given for Al. However there is very little experimental data available on the skin depth in Sn at microwave frequencies. The

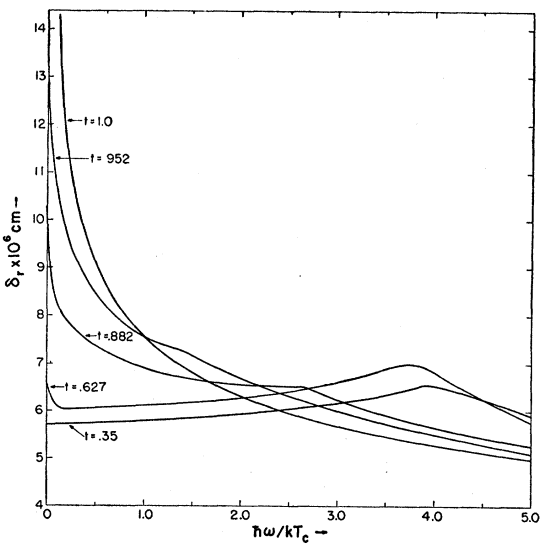

FIG. 10. The theoretical skin depth of Sn is plotted versus reduced frequency, for various values of the reduced temperature.

final numerical results for Sn have assumed the BCS value of $E_g(0)=3.53kT_c$.

ACKNOWLEDGMENTS

I thank Professor John Bardeen for suggesting this problem and for his valuable guidance in this work. I also thank G. Rickayzen, A. H. Nethercot Jr., K. T. Rogers, and T. Tsuneto for valuable discussion. I also thank R. Kaplan, A. H. Nethercot Jr., and H. A. Boorse as well as M. A. Biondi and M. P. Garfunkel for permission to use their results prior to publication.

PHYSICAL REVIEW VOLUME 118, NUMBER 4 MAY 15, 1960

Varley Mechanism for Defect Formation in Alkali Halides*

D. L. DEXTER
University of Rochester, Rochester, New York
(Received December 2, 1960)

The Varley mechanism is examined, according to which Frenkel defects are produced in the halogen sublattice of alkali halides subsequent to multiple ionization of the halide ions. Arguments are presented to show that the lifetime of a positive halogen ion against recapture of electrons in orders of magnitude smaller than the ejection time of the halogen, and thus that the Varley mechanism is inoperative. The arguments may not be applicable for inner shells alone, but experimental evidence is adduced to eliminate this case.

THE so-called Varley mechanism[1] for the x-ray production of interstitial halogen, negative-ion vacancies, and F centers in alkali halide crystals has recently been receiving increasing attention. This proposed mechanism postulates the multiple ionization of a halide ion in its normal position surrounded by positive alkali ions, thus resulting in the presence of a *positive* halogen ion in a region of high-electrostatic (Madelung) potential, from which the halogen may be ejected under the influence of lattice vibration. This would give rise to the presence of interstitial halogen and negative-ion vacancies, which could easily trap electrons to become F centers. There are indications from experiments on multiple ionization in rare gases that if the Varley mechanism were the only one operative, a sizable fraction of multiple ionization events in alkali halides would have to result in the production of F centers, in order to be consistent with the efficiency of coloration at low temperatures.

Though no direct evidence has been adduced for this mechanism, it has increasingly been invoked because of its apparent consistency with low-temperature experiments for which most other mechanisms seem inappropriate.

Howard and Smoluchowski[2] have commented on some of the critical factors involved in this mechanism, one of which is the lifetime of the positive halogen ion against recapture of an electron from the conduction band, and they estimate this quantity in terms of the concentration and mobility of free electrons. They conclude that if the electron concentration in the conduction band is $\lesssim 10^{17}$ cm^{-3}, the probability for recapture of one electron (sufficient, in the case of *double* ionization, to "turn off" the Varley mechanism) is less than 10^{12} sec^{-1}, the reciprocal of which, they suggest, is a reasonable characteristic time for the ejection of a positive halogen ion from its lattice site.

The above views are seen to be expressed in terms of a "hard billiard ball," or "*very* tight binding" approximation, as if the removed electrons can be localized on a particular lattice site. The purpose of this note is to point out that if this extreme point of view is relaxed, another and far more probable mechanism exists in many cases for rendering inoperative the Varley mechanism.

In the tight-binding approximation, when we allow for a nonzero overlap of neighboring halogen wave functions, so as to give a nonzero width to the valence band, we suspect that in a very short time an electron will be "sucked" by the strong Coulomb field to the postulated positive halogen ion from an adjacent halide ion, thus producing two adjacent halogen atoms. (This initial transition, which in itself is sufficient to render inoperative the Varley mechanism, could be followed by other jumps of electrons, further separating the neutral halogen atoms.) The initial jump time will of course depend on the extent of overlap, and if the latter is not zero, the former is not infinite. This point of view, while suggestive, does not easily allow a computation of the original jump time nor a description of what happens to the original large potential energy.

These questions are readily answered, at least in part, on going to an energy-band picture. In this description we would say that double ionization corre-

* Research supported in part by the U. S. Air Force Office of Scientific Research of the Air Research and Development Command.

[1] J. H. Varley, Nature **174**, 886 (1954); J. Nuclear Energy **1**, 130 (1954).

[2] R. E. Howard and R. Smoluchowski, Phys. Rev. **116**, 314 (1959).